A new approach to depict bone surfaces in finger imaging using photoacoustic tomography

S. K. Biswas [†a, b] , P. van Es [†a] , W. Steenbergen[a], S. Manohar[*]
[a]Biomedical Photonic Imaging, University of Twente, P. O. Box 217, 7500 AE, Enschede, The Netherlands; [b]Department of Instrumentation and Applied Physics, Indian Institute of Science, Bangalore 560012, India
[†]Equal contribution

ABSTRACT

Imaging the vasculature close around the finger joints is of interest in the field of rheumatology. Locally increased vasculature in the synovial membrane of these joints can be a marker for rheumatoid arthritis. In previous work we showed that part of the photoacoustically induced ultrasound from the epidermis reflects on the bone surface within the finger. These reflected signals could be wrongly interpreted as new photoacoustic sources. In this work we show that a conventional ultrasound reconstruction algorithm, that considers the skin as a collection of ultrasound transmitters and the PA tomography probe as the detector array, can be used to delineate bone surfaces of a finger. This can in the future assist in the localization of the joint gaps. This can provide us with a landmark to localize the region of the inflamed synovial membrane. We test the approach on finger mimicking phantoms.

Keywords: photoacoustic computed tomography, ultrasound, bone delineation, joint gap, finger, rheumatoid arthritis

1. INTRODUCTION

Rheumatoid arthritis (RA) is a chronic joint disease that causes disability due to swelling, stiffness, pain and progressive joint destruction.[1] It's estimated that 1-3% of the population suffers from a reduced quality of life due to RA. Inflammation of the synovial membrane or synovitis is an indicated as a marker of the ongoing degradation process of cartilage and adjacent bone. The inflammation is process is also characterized by angiogenesis at the synovial membrane which causes the generation and relocation of blood vessels.

Current strategies to treat RA include anti-inflammatory and conventional or biological immunosuppressive drugs. Photoacoustic (PA) tomography has potential in the diagnosis and monitoring of inflammatory diseases such as rheumatoid arthritis (RA). The technique utilizes short nanosecond light pulses that lead to thermoelastic expansion and the emission of ultrasound waves from light absorbing structures such as blood vessels. These emitted ultrasound waves can be registered in time and used to visualize the position of blood vessels. Changes in the vasculature of the inflamed synovial membrane, which is located around the joint gap, might therefore be depicted in high detail in RA patients.

Due to wavelength specific absorption of laser light by chromophores in tissue, PA can gather both functional and molecular absorption information. This, at depths much larger than the optical transport mean-free path of biological tissue and at the resolution of ultrasound imaging. The capabilities of PAT are however limited to tissue structures containing chromophores with an absorption coefficient, in the visible and (near-) infrared (NIR) range, higher than the absorption coefficient of the surrounding tissue. Structural imaging of bone and tendons is for instance challenging with PA imaging. Typically, other imaging modalities such as ultrasound imaging (US), computed tomography (CT) and magnetic resonance imaging (MRI) do have the ability to visualize these structures.

*s.manohar@utwente.nl; University of Twente, TNW, Biomedical Photonic Imaging, Drienerlolaan 5, Enschede, The Netherlands, 7522DB; phone +31-(0)53-4893164; fax +31-(0)53-4891105; www.utwente.nl/bmpi/

Photons Plus Ultrasound: Imaging and Sensing 2015, edited by Alexander A. Oraevsky, Lihong V. Wang
Proc. of SPIE Vol. 9323, 932322 · © 2015 SPIE · CCC code: 1605-7422/15/$18
doi: 10.1117/12.2078703

Photoacoustic imaging is used in the field of breast imaging [2-4], melanoma metastasis detection in sentinel lymph nodes [5]and intravascular imaging but has many more applications in small animal imaging as it also allows *in vivo* monitoring of endogenous and exogenous markers in a wide variety of disease models.

Recent work from our group that focusses on imaging vasculature in the healthy finger showed the feasibility of making detailed transversal cross-section images of the finger vasculature at a resolution up to 100um.[6] It also showed the presence of strong reflection artifacts from epidermal PA signals that were scattered at the surface of the bone (Figure 1(a) white arrow). Fortunately these artifacts were primarily visible within the boundaries of the bone surface and did not interfere with the PA signals of vascular structures around it. One interesting observation was that the intensity of these reflection artifacts seemed to be reduced at the estimated location of joint gap. However, the exact location of the joint gap was difficult to identify from the PA images without additional coregistration of conventional ultrasound images. Additionally, the interpretation of vasculature close to the bone surface is often challenging in PA imaging because it is difficult to distinguish vasculature from reflection artifacts in the same region.

The generation of these artifacts in PA images is visualized schematically in Figure 1(b). The PA signals from a PA source, such as the epidermis, either travel over the shortest distance x_{sd} towards the detector (blue arrows) or travel the distance $x_{sb} + x_{bd}$ which is the sum of the distance from PA source to the bone and the distance from bone to the detector (red arrows). During reconstruction the reflected signals from the PA source will cause an artifact at a distance of $x_{sb} + x_{bd}$ from the detector as shown as a red dot in the image.

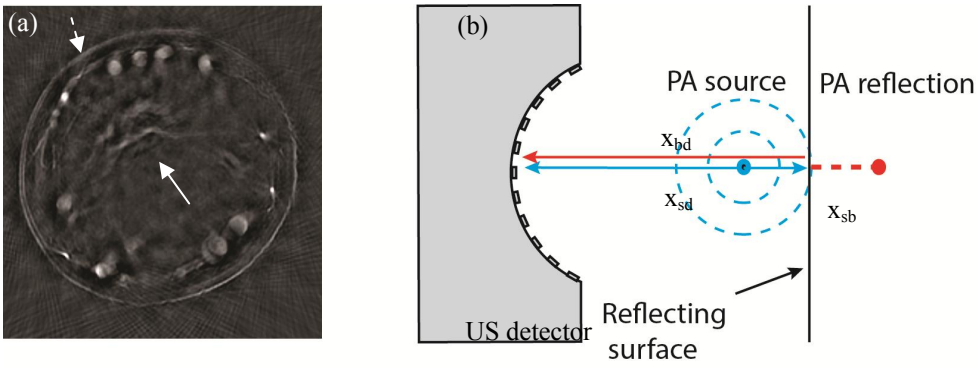

Figure 1: (a) Photoacoustic cross-section image of the finger showing the epidermis (dashed arrow), blood vessels (circles beneath the epidermis), and reflection artifacts (white arrow). These artifacts are originating from the epidermis and blood vessels. (b) Schematic drawing explaining the cause of the artifacts. A PA source such as the epidermis generates acoustic signals towards the detector and towards a reflecting surface. The signals directly traveling towards the detector arrive first. The reflected signals travel towards to detector with a delay due to the the distance ($x_{sb} + x_{bd}$). A photoacoustic reconstruction algorithm projects the measured intensities back to the wrong position at the distance ($x_{sb} + x_{bd}$).

We now show that a conventional ultrasound reconstruction algorithm, that considers the skin as a collection of ultrasound transmitter and the PA tomography probe as the detector array, can be used to delineate surfaces of a finger's bone and therefore assist in the localization of the joint gap. The benefit of these echogenicity maps is that these have been produced by endogenously generated PA signals that interrogate the tissue. Due to the perfect match in time registration and ultrasound receiver locations, we are able to show co-registered PA and so called: photoacoustically-induced ultrasound (PAUS) images. We test the method on cylindrical finger mimicking phantoms with bone mimicking objects inside..

2. MATERIALS AND METHODS

2.1. Setup

Imaging of the finger was performed by our previously discussed photoacoustic computed tomography setup.[6, 7] The water tank holds a 32-element curvilinear ultrasound array (Imasonic, Besançon, France) and 6 fiber bundles pointing towards the center (Figure 2(a)) The whole ensemble can rotate 360 degrees around the object under investigation and then subsequently moves down along the object to collect a stack of sliced PA images. The 6 optical fiber bundles, which were evenly distributed in a half circle around the sample, have a 4 mm diameter and a NA of 0.22. These provided backward-mode illumination of 6 contiguous round spots of 11 mm with roughly a top-hat energy distribution at the object surface. The 6ns laser pulses are generated by a combination of a Nd:YAG laser (Quanta-Ray pro 250, @10 Hz, Spectra Physics, Mountain View, CA) pumping an OPO (VersaScan- L532, GWU, Germany). All photoacoustic signals were detected by an array of 32 piezoelectric elements that are equally spaced over a radius of curvature of 40 mm. The piezocomposites have a center frequency of 6.25 MHz and a -6 dB bandwidth of over 80%. Based on a total amount of 12 view angles around the object we measured an in-plane resolution of 100 µm for this PA system. In the elevational plane, the elements are focused mechanically at a distance of 48 mm which resulted in a -3 dB focus of roughly 1 mm in the elevational plane. For data acquisition a 32-channel pulser/receiver (Lecoeur-Electronique, Chuelles, France) sampling at 80 MSs^{-1} was used.

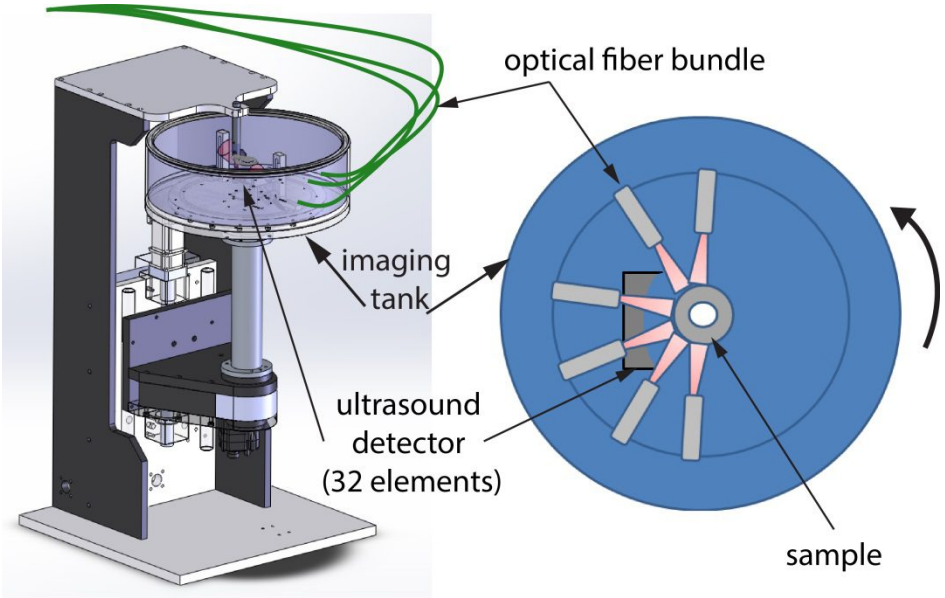

Figure 2: Schematic drawings of the photoacoustic setup. Six optical fibers excite the phantom with pulsed laser light. The 32 detector elements receive photoacoustic signals along the perimeter of the sample. The imaging tank with optical fiber bundles and ultrasound detector rotates around the finger or finger phantom.

2.2. Experimental phantom models

Several agar-based phantoms representing simplified models of bone and epidermis containing fingers were fabricated to evaluate the feasibility of delineating the bone surfaces by PAUS imaging. Bone simulating acoustic reflectors (Figure 2) in the shape of a circular rod and a roughly elliptical cross-sectional rod, were fabricated from Delrin® to mimick bone structures. A third acoustic reflector was the index finger of a skeleton hand model (Labor ActivA B.V, EZ6003, Steenbergen, The Netherlands).

The acoustic reflectors were subsequently embedded in a 3 wt% agar gel with a diameter of 20 mm (P1) or 26 mm (P2) containing 1% Intralipid® (20%, Fresenius-Kabi Netherlands BV, Zeist, The Netherlands) to mimic a scattering tissue. For the finger phantom (P3), the agar gel was fashioned to take the dimensions of a finger around the bone. In order to simulate a thin melanin layer such as encountered in the epidermal skin layer, the agar cylinders were dipped shortly into a 1 wt% mobile agar gel (40 °C) solution containing 600 µl of India Ink® (supplier, location) per 500ml water and, immediately afterwards, dipped in ice water (0 °C) which resulted in a highly absorbing dye layer of (200-500µm) around the cylinders.

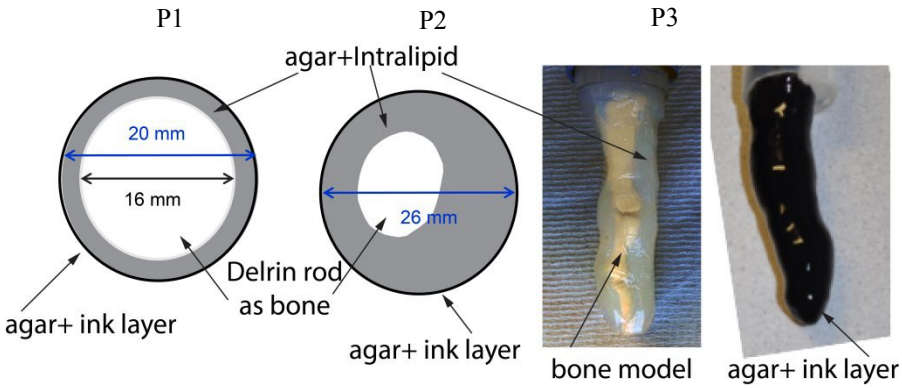

Figure 3: Schematic drawings of the phantoms developed from left to right P1, P2 and P3. Bone simulating acoustic reflectors of Delrin are used in P1 and P2. For P3 a finger of skeleton hand model is used. These acoustic reflectors are embedded in agar gel with Intralipid for scattering and a surface absorbing layer based on agar and ink.

2.3. Phantom measurements

All phantoms were measured with 12 projections or view angles with 30 degrees spacing. The imaging time per slice was approximately 60 seconds

2.4. Image reconstruction

The reflection artifacts in the finger are predominantly coming from those PA signals that are generated by epidermis and are reflected on the bone surface. For this situation, when defined as conventional (reflection mode) US imaging, we can assign the skin as an array of ultrasound transmitters along the finger circumference that probes/excites the finger tissue with ultrasound waves. These PAUS waves can be detected by the ultrasound detectors when reflected on the bone surface.

This works in a similar way as laser-induced ultrasound (LUS) sources for reflection-mode ultrasound imaging.[8-11] In our case, no external ultrasound source was used to generate the ultrasound. Instead, we used the endogenous chromophore melanin, which is abundantly present in the epidermis, as PAUS source.

PA images were reconstructed using a simple acoustic filtered back-projection algorithm. Details can be found in Ref. 6. The PAUS algorithm uses the detected epidermis (surface) locations and projects the measured intensities from the ultrasound detectors to discrete points in the PAUS map and back to the epidermis locations.

The PAUS algorithm exploits the fact that the curvature of our probe allows reconstruction with one pulser/receiver pair that are in one line towards the mechanical center of rotation of the setup. This line is approximately perpendicular to the epidermis in most cases due to the circular symmetry of both the probe and finger. This can be regarded as the analogue of line/A-scan imaging at multiple locations around a circular object and is highly selective for surfaces of acoustic scatterers that run parallel to the skin surface. Details can be found in Ref 12.

All PA images are plotted in a linear grayscale. The PAUS images were plotted at a logarithmic scale for which we manually picked a suitable threshold level to visualize the acoustic scatterers.

3. RESULTS

3.1. Bone delineation

Figure 4 show the PA images of the phantom P1 and P2 respectively in column 1. The circular shape of the absorbing ink layer at the surface of all agar gel phantoms is clearly visible. Artifacts caused by acoustic reflections of ink layers PA signal on the Delrin® samples are visible inside the phantoms From the PA images of each phantom the location of the ink layers was detected and defined as a collection of discrete PAUS sources, the images were reconstructed using the proposed algorithm.

Column 2 of Figure 4 show the images made by PAUS for the two bone mimicking objects. The darker lines depict the shapes of the acoustic reflectors inside the agar cylinder. (Note the image data has been complemented, to form a negative of the image, to highlight the bone.)

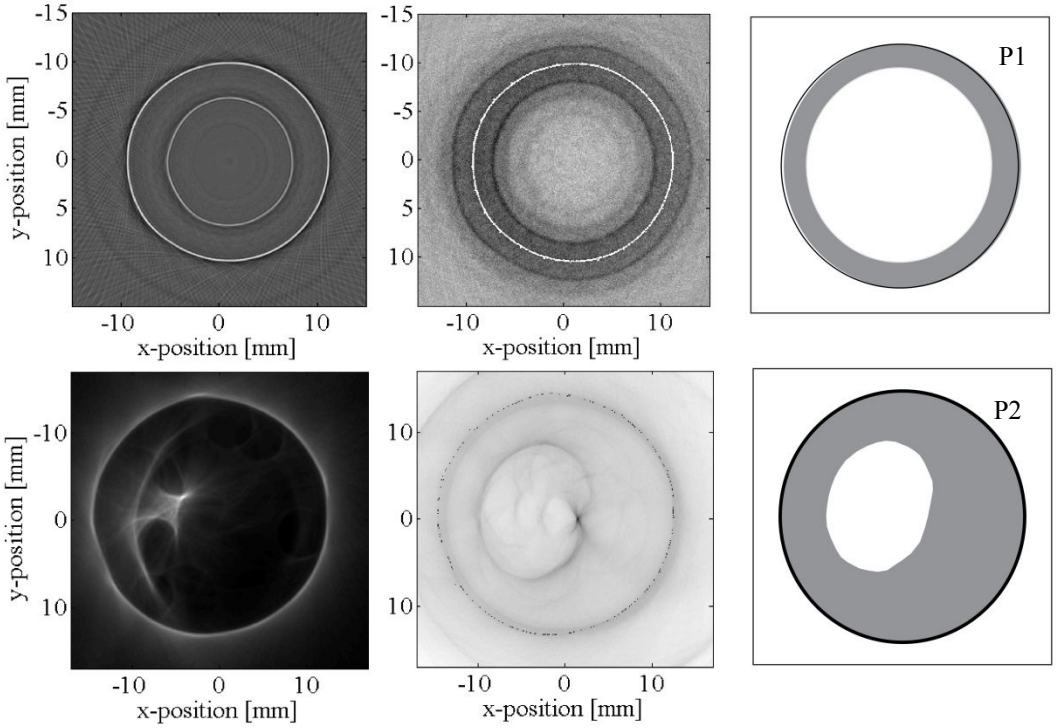

Figure 4: First column: PA images of finger phantoms P1 (row1) and P2 (row2). The ink layer that represents the skin of a finger is shown as a white circle. The photoacoustically induced ultrasound (PAUS) from the ink layer is reflecting on bone simulating objects which causes artifacts inside the PA image. Second column: PAUS images that show the approximate locations of reflecting surfaces of the two bone objects. Third column: Schematics of the phantoms (P1 and P2) carrying bone objects.

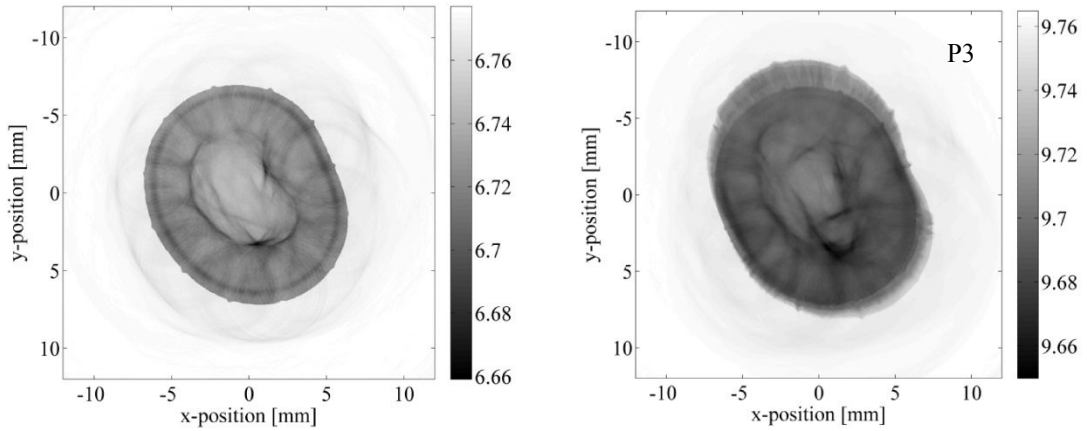

Figure 5: The photoacoustically induced ultrasound (PAUS) image of P3 in two slices.

Figure 5 shows two slices of the PAUS reconstruction where the bone mimicking object's surface can be visualized. (Note that the image data has been complemented, to form a negative of the image, to highlight the bone.)

4. DISCUSSION AND CONCLUSION

Results from phantom and *in vivo* data show that PAUS imaging is feasible with the epidermis as endogenous photoacoustic source. For three finger phantoms we have shown to be able to delineate the location of the bone surfaces. Although the accuracy of the delineation is not as rigorously accurate as in conventional ultrasound imaging, it does allow the visualization of the approximate bone surface location. This approach can in the future assist in the localization of the joint gaps using PA data from a CT geometry. The location of the joint gaps can provide a landmark to localize the region of the inflamed synovial membrane.

As the implemented algorithm was the basic back-projection algorithm, which is often used but less accurate than more recent US reconstruction algorithms, we expect that image quality can be significantly improved in future research. Improvements in our back-projection algorithm can be made by taking into account the directionality of the focused propagating photoacoustic waves and by including the receive aperture of the ultrasound detectors.
PAUS image reconstruction might in the future also be performed by iterative algorithms. This will reduce the amount of back projection artifacts (streaks) that are currently present in our reconstructions.

In conclusion, we introduced PAUS imaging with the epidermis as endogenous ultrasound source. These coregistered images will help the interpretation of PA images by identifying the location of an acoustic scatterer such as bone in finger joints.

REFERENCES

[1] Alamanos, Y., and Drosos, A. A., "Epidemiology of adult rheumatoid arthritis," Autoimmunity rev, 4(3), 130-6 (2005).

[2] Heijblom, M., Piras, D., Xia, W. *et al.*, "Visualizing breast cancer using the Twente photoacoustic mammoscope: What do we learn from twelve new patient measurements?," Opt. Express, 20(11), 11582-11597 (2012).

[3] Kitai, T., Torii, M., Sugie, T. *et al.*, "Photoacoustic mammography: initial clinical results," Breast Cancer, 21(2), 146-153 (2014).

[4] Kruger, R. A., Kuzmiak, C. M., Lam, R. B. *et al.*, "Dedicated 3D photoacoustic breast imaging," Med Phys, 40(11), 113301 (2013).

[5] Jose, J., Grootendorst, D. J., Vijn, T. W. *et al.*, "Initial results of imaging melanoma metastasis in resected human lymph nodes using photoacoustic computed tomography," j Biomed Opt, 16(9), 096021-096021-5 (2011).

[6] Van Es, P., Biswas, S. K., Bernelot Moens, H. J. *et al.*, "Initial results of finger imaging using photoacoustic computed tomography," J Biomed Opt, 19(6), 060501 (2014).

[7] Jose, J., Willemink, R. G. H., Steenbergen, W. *et al.*, "Speed-of-sound compensated photoacoustic tomography for accurate imaging," Med Phys, 39(12), 7262-7271 (2012).

[8] Nuster, R., Schmitner, N., Wurzinger, G. *et al.*, "Hybrid photoacoustic and ultrasound section imaging with optical ultrasound detection," J Biophotonics, 6(6-7), 549-59 (2013).

[9] Wurzinger, G., Nuster, R., Schmitner, N. *et al.*, "Simultaneous three-dimensional photoacoustic and laser-ultrasound tomography," Biomed Opt Express, 4(8), 1380-1389 (2013).

[10] Deán-Ben, X. L., Ntziachristos, V., and Razansky, D., "Artefact reduction in optoacoustic tomographic imaging by estimating the distribution of acoustic scatterers," J Biomed Opt, 17(11), 110504-110504 (2012).

[11] Fehm, T. F., Deán-Ben, X. L., and Razansky, D., "Four dimensional hybrid ultrasound and optoacoustic imaging via passive element optical excitation in a hand-held probe," Appl Phys Lett, 105(17), - (2014).

[12] Biswas, S. K., Van Es, P., Steenbergen, W. and Manohar, S., "A method for delineation of bone surfaces in photoacoustic computed tomography of the finger," (2015) (under review)